

## Electrical Repulsive Energy between Two Cylindrical Particles with Finite Length: Configuration Dependence

Juyoung Choi, Hyunbae Dong, Seungjoo Haam, and Sang-Yup Lee\*

Department of Chemical Engineering, Yonsei University, Seoul 120-749, Korea. \*E-mail: leessy@yonsei.ac.kr

Received February 5, 2008

The electrical repulsive energy between two model cylinders was calculated by solving nonlinear Poisson-Boltzmann (P-B) equation under Derjaguin approximation. Effects of the surface potential, Debye screening length, and configuration of cylinders on the repulsive interaction energy were examined. Due to the anisotropy of the shape of cylinder, the interaction repulsive energy showed dependence to the configuration of particles; cylinders aligned in end-to-end configuration showed largest repulsive energy and crossed particles had lowest interaction energy. The configuration effect is originated from the curvature effect of the interacting surfaces. The curved surfaces showed less repulsive energy than flat surfaces at the same interacting surface area. The configuration dependency of interaction energy agreed with the previous analytical solution obtained under the linearized P-B equation. The approach and results present in this report would be applicable in predicting colloidal behavior of cylindrical particles.

**Key Words:** Electrical repulsion, Derjaguin approximation, Orientation, Cylinder

### Introduction

Calculation of the electrostatic interaction between anisotropic colloidal particles suspending in an aqueous ionic solution is a complex problem to solve. Though many anisotropic particles suspending in an aqueous medium such as synthetic nanorod<sup>1,2</sup> and natural biomolecular suspensions<sup>3,4</sup> have been exploited for the engineering and medical applications, the analysis on the colloidal interaction between these particles has not fully understood yet. There are several difficulties in analyzing the electrostatic interaction of anisotropic particles; firstly, the electrostatic interaction is dependent to the configuration because of the anisotropic structure of interacting particles. Secondly, the governing equation of Poisson-Boltzmann equation (P-B equation) has inherent complexity with nonlinearity.<sup>5,6</sup> Thirdly, the surface charge density of anisotropic particle changes with the gradient of electrostatic potential at the surface. Thus, the charge density is not even on the anisotropic surfaces.<sup>7</sup>

Among many anisotropic colloidal particles, the cylindrical particles such as nanorods and nanotubes have attracted special interest because these cylindrical particles are promising materials for the fabrication of future devices. To fabricate these colloidal cylindrical particles, analysis on the interaction energy between them is necessary. Analyses on the electrostatic interaction between cylindrical particles aligned in parallel have been carried out during last decades.<sup>8-11</sup> In the previous studies, the electrostatic repulsion between two parallel cylinders were calculated under the assumption of linearized P-B equation with thin Debye screening length in comparison to the radius of the cylinder. This assumption is valid only for a system of colloidal cylindrical particles with a low surface potential (in general,  $\leq 25$  mV at 25 °C) suspending in a highly concentrated ionic solution system whose Debye screening length is much

smaller than radius of cylinder. The limitation of linearized P-B equation and low surface potential was overcome by introducing numerical technique. The numerical solution of nonlinear P-B equation enabled to analyze the interacting forces without above limits in more complex systems. By using bycylinder coordinates, the interaction free energy between two parallel cylinders with infinite length was solved numerically.<sup>12</sup> Another rigorous numerical study on the interaction energies between parallel cylinders with infinite length confined in a rectangular channel was reported by Ospeck and Fraden.<sup>13</sup> In their study, the variation of electrostatic repulsive force by the constriction of rectangular wall was calculated using finite element method (FEM). All of these studies were carried out for a system of infinite cylinders aligned in parallel. However, the parallel configuration is not sufficient to describe every possible colloidal interaction between two cylinders because enormous configurations can be made.

Interaction energy with the consideration of interparticle configuration of two cylinders was analytically solved by Halle.<sup>6</sup> Four canonical configurations of two cylinders were defined, and electrostatic repulsive energies of each configuration were calculated with the variation of separation distance. The analytical solution was expressed as an integration form in the function of linear charge density. However, in deriving above analytical solution, linearized P-B equation and linear charge density on the cylindrical particle were hypothesized. Due to these assumptions, the obtained solution was valid only when the cylinder has low surface potential and the interacting particles were separated far enough. Therefore, the result was not applicable when the particles strongly interact each other in a short distance. When the highly charged surfaces were positioned close with each other, the electrical double layers were overlapped. This overlapping makes the interaction complex to analyze. As far as we

know, there is no analytical or numerical solution of the electrical interaction energy between two cylindrical particles with the considerations of nonlinear P-B equation and configurations to date.

In this work, the electrical repulsive energies between two cylindrical particles are calculated numerically with the considerations of the high surface potential, electrical double layer overlapping, and configurations. For the calculation, four canonical configurations were defined and Derjaguin approximation (as known as Derjaguin integration method) was applied. Using the Derjaguin approximation, the electrical potential distribution between interacting surface elements were obtained while the surface potential and Debye screening length were chosen as parameters. From the electrical potential distribution, the repulsive energy was calculated by considering osmotic pressure between surface elements. Since the Derjaguin approximation offers reasonable results when the interparticle distance is close enough, this approach would be valid for the conditions where the cylindrical particles were positioned closely. Thus, numerical approach would overcome the previous limitation of the conditions of strong surface potential, thick Debye screening length, and the short separation distance. This result is expected to be applicable in analyzing many colloid application systems such as liquid crystal, nanotubes, and colloidal nanorods.

### Modeling of the System

In Figure 1, four canonical configurations were present. For a specific configuration, the interacting surfaces were defined as the orthogonally projected area of one cylinder to the other. The shadowed area in Figure 1 represents the interacting surfaces. Derjaguin integration method was applied between these interacting surfaces. The Derjaguin approximation is useful in calculating electrical potential distribution between surfaces with complex geometries.<sup>14</sup> When applying Derjaguin approximation, the cylindrical particle surfaces were differentiated to discrete surface elements, and

then corresponding surface elements were determined. The potential distribution between corresponding surface elements was calculated using finite element method. As the potential distribution is governed by nonlinear P-B equation, the numerical approach for the potential distribution is necessary. In calculating the electrostatic potential distribution, several assumptions were introduced. Firstly, the cylinders have same charge with constant surface potential. This constant surface potential condition is easily applicable to the real colloidal system in which the surface potential was approximated by the zeta potential of the particles of interest. The condition of constant surface potential is valid when the particles were charged by the adsorption of ions to the surface<sup>15</sup> though the surface charge and charge density would vary self-consistently in practice due to the dynamic equilibrium of ions. Secondly, the interaction energy was assumed to be independent to the particle concentration. From a previous experimental study on the electrophoresis of cylindrical colloidal particles, the interaction energy was not influenced by neighboring particles under a critical concentration.<sup>16</sup> Thus, this assumption is valid when the particle concentration is low enough so that influence of neighboring particle can be ignored. Thirdly, the dielectric constant of the cylinder is assumed to be zero not to consider the potential distribution inside of the cylindrical particles. This assumption is valid many polymeric and biomolecular particles with low dielectric constant. Finally, the end effect of cylindrical particles was ignored in every calculation for the simplicity.

Canonical configurations of two cylindrical particles were defined in the same way as Halle suggested.<sup>6</sup> The factors defining the configuration of particles are separation distance between particles, three angles, and the length of the cylindrical particles. In this study the lengths of cylindrical particles were set as  $L$  and the particles were aligned along to the symmetric axis. The four characteristic configurations were labeled as  $H$ ,  $I$ ,  $T$ , and  $X$  configurations, respectively. The schematic layout of the canonical configuration is present in Figure 1.

After determining the configuration of cylindrical particles, the whole interacting cylindrical particle surfaces were differentiated to planar surface elements. The electrical potential profile and the repulsive energy between these interacting planar surface elements were numerically calculated. The repulsive energy between each differential element was calculated from the potential profile, and then the total repulsive energy was obtained by integrating the each repulsive energy working between surface elements. In Figure 2, a schematic diagram of interacting surface elements in the crossed ( $X$ ) configuration is present. A differential surface element of one cylinder and corresponding surface element of the other cylinder is separated with a distance of  $h$ . The total interacting surface of one cylinder is marked as a shadow area. Each cylindrical particle has radius,  $a$ , and length,  $L$  with shortest separation distance of  $d$ . The cylindrical wall of the particles was divided by  $30 \times 30$  differential surface elements in calculation. For the crossed configuration, the surface area is set as

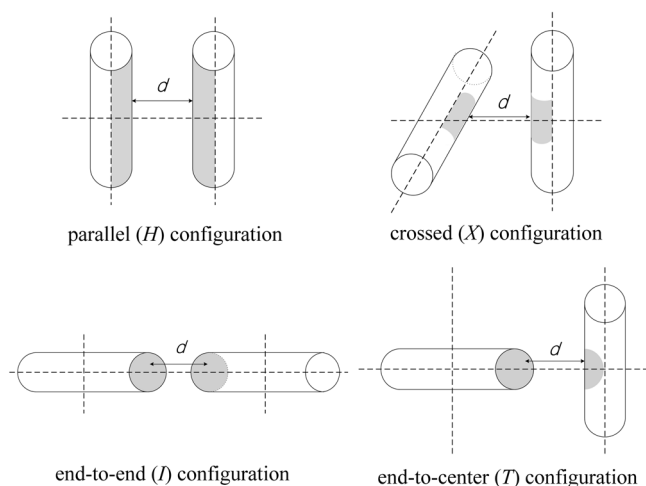


**Figure 1.** Four canonical configurations of two finite cylindrical particles.

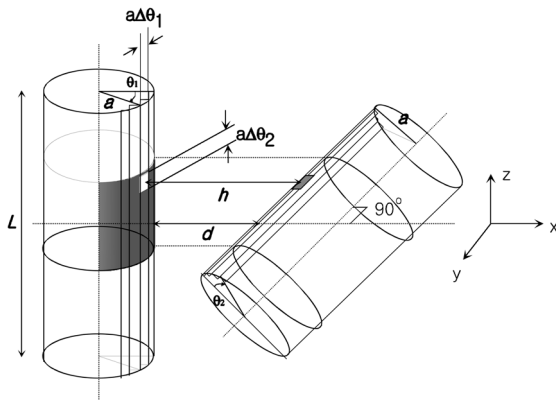


**Figure 2.** Schematic diagram of interacting surface elements between two cylindrical particles in the crossed ( $X$ ) configuration.  $d$  is the shortest separation distance and  $h$  is the distance between interacting surface elements.

$$\Delta S = a \sin \Delta \theta_1 \sin \Delta \theta_2 \approx a^2 \Delta \theta_1 \Delta \theta_2 \quad (1)$$

and the separation distance is

$$h = \frac{d + 2(a - \cos \theta_1 - \cos \theta_2)}{a} \quad (2)$$

For the other configurations, a similar approach has been carried out.<sup>17</sup>

Once the configuration and surface elements were determined, the electrical potential profile between surface elements is calculated which is represented by the nonlinear P-B equation. In a colloidal system with monovalent (1:1) electrolytes, the P-B equation is expressed as follows;

$$\nabla^2 \psi = \frac{2F_a C_\infty}{\epsilon_0 \epsilon_r} \sinh\left(\frac{F_a \psi}{RT}\right) \quad (3)$$

where,  $F_a$  is faraday constant,  $C_\infty$  is bulk ion concentration in mole/L,  $\epsilon_0$  is vacuum permittivity, and  $\epsilon_r$  is relative permittivity of suspending medium.<sup>18</sup> By applying Derjaguin approximation, the P-B equation can be simply expressed in the rectangular coordinates present in equation (4).

$$\frac{d^2 \psi}{dx^2} = \frac{2F_a C_\infty}{\epsilon_0 \epsilon_r} \sinh\left(\frac{F_a \psi}{RT}\right) \quad (4)$$

Above P-B equation can be expressed in the dimensionless form by introducing dimensionless parameters that are defined as

$$\tilde{\psi} = \frac{F_a \psi}{RT} \quad \text{and} \quad y = \frac{x}{a} \quad (5)$$

respectively.

The dimensionless form of P-B equation of (4) is

$$\begin{aligned} \frac{d^2 \tilde{\psi}}{dy^2} &= a^2 \frac{2F_a^2 C_\infty}{\epsilon_0 \epsilon_r RT} \left\{ \frac{e^{\tilde{\psi}} - e^{-\tilde{\psi}}}{2} \right\} \\ &= \frac{1}{2} \frac{a^2}{\lambda_D^2} (e^{\tilde{\psi}} - e^{-\tilde{\psi}}) \end{aligned} \quad (6)$$

where,  $\lambda_D$ , the Debye screening length, is defined as follows.

$$\frac{1}{\lambda_D^2} = \kappa^2 = \frac{2F_a^2 C_\infty}{\epsilon_0 \epsilon_r RT} \quad (7)$$

The dimensionless forms of boundary conditions of constant surface potential,  $\psi_0$ , are to be applied to solve equation (6) present in equation (8).

$$\tilde{\psi} = \tilde{\psi}_0 = \frac{F_a \psi_0}{RT} \quad \text{at} \quad h = 0 \quad \text{and} \quad h = \frac{d + 2(a - \cos \theta_1 - \cos \theta_2)}{a} \quad (8)$$

By solving equation (6) with the boundary conditions of (8), the potential distribution between differential surface elements could be obtained. From the potential distribution, the repulsive energy can be stated as a function of the potential at the middle position,  $\psi_m$ . The repulsive energy working between surface elements,  $\Delta V_r$ , is present as a function of dimensionless middle position potential,  $\tilde{\psi}_m$ .

$$\Delta V_r = \int_h^\infty 2C_\infty RT \{ \cosh(\tilde{\psi}_m) - 1 \} dx \quad (9)$$

In deriving equation (9), Maxwell stress was ignored since the potential profile was symmetric. Finally, the  $\Delta V_r$  of each differential surface element was summarized to calculate total repulsive energy.

To obtain the potential profile from the nonlinear P-B equation, numerical method was applied. Equation (6) was solved using Gelakin finite element method (G/FEM) with quadratic basis functions. Newton's method was applied until the potential values are converging under the tolerance of  $1 \times 10^{-4}$ . From the potential profile, the middle point potential,  $\psi_m$ , was determined, and then the repulsive energy between surface elements was calculated in sequence.

## Results and Discussion

Electrical interaction energy between cylindrical particles is subject to the configurations of particles since the interacting surface area and mean separation distance change with respect to the configuration. In general, the larger and the closer interacting surface area would result in higher repulsive energy, while longer separation distance reduces the repulsion. The curvatures and interacting surface area change with respect to the configuration. These interacting area and curvature changes would alter the interaction energy. The repulsive energies were calculated with the separation distance between  $d/a = 0.0$  and 1.0 because the Derjaguin approximation is valid only when the separation distance is comparable to the curvature of the interacting surface.<sup>19,20</sup>

In Figure 3, the repulsive energy of cylindrical particles in the parallel ( $H$ ) configuration is plotted against the dimensionless Debye screening length,  $\kappa a$ , with parameters of dimensionless surface potential. In calculation, the cylinder length of  $L$  was chosen as  $a$ , same to the radius of cylinder in order to express the repulsive energy in terms of dimensionless unit length of the cylinder. The interacting surface area

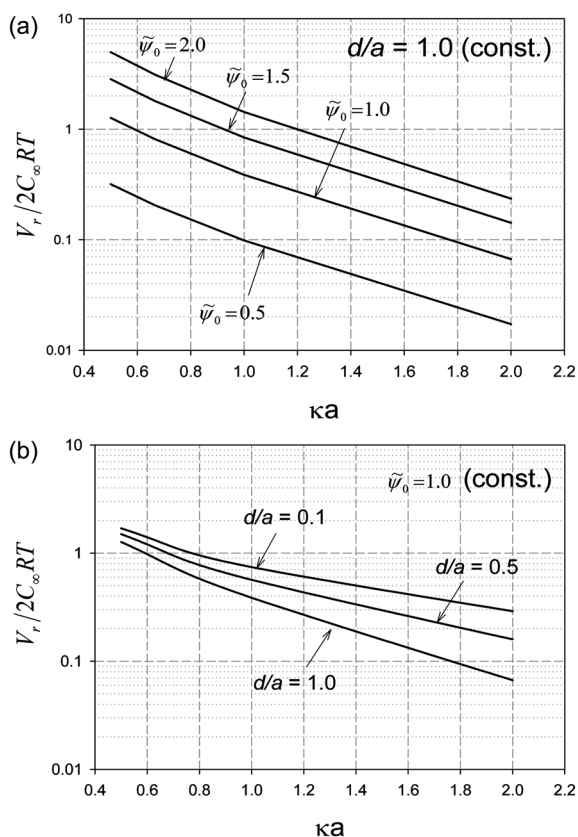


**Figure 3.** Repulsive energy change between parallel cylindrical particles ( $H$  configuration); (a) at constant separation distance of  $d/a = 1.0$  with surface potential changes, (b) at constant surface potential of  $\tilde{\psi}_0 = 1.0$  with separation distances.

is  $2a^2$ . The repulsive energy is plotted at a constant separation distance of  $d/a = 1.0$  in Figure 3(a). The higher surface potential, the larger repulsive energy was obtained at a constant Debye screening length. It is obvious that the electrical repulsion would increase as the surface potential of interacting particles increases. At a constant surface potential, thicker Debye screening length resulted in higher repulsive energy. The increase of Debye screening length leads to overlapping of electrical double layers around the cylindrical particles resulting in higher repulsion. In figure 3(b), the repulsive energy at a constant surface potential of  $\tilde{\psi}_0 = 1.0$  with the variation of the separation distance is present. The repulsive energy decayed as the separation distances were extended and Debye screening length decreased. Decay of repulsive energy is reasonable considering that the overlapping of electrical double layers would be weakened as the interacting cylinders were separated apart. All of these repulsion energy dependences to the surface potential, separation distance, and Debye screening length were commonly observed in every canonical configuration.

Repulsive energy working between cylindrical particles in the end-to-end ( $I$ ) configuration is shown in Figure 4. In this configuration, the interacting surfaces are the parallel circular cross section of cylinders, and the separation distance of surface elements,  $h$ , is always consistent with the separation distance,  $d$ . The repulsive energy increased with Debye

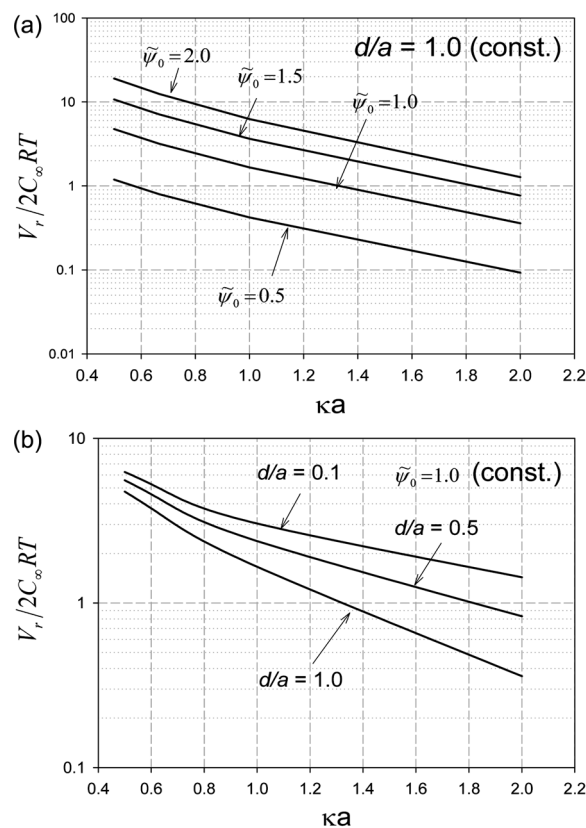


**Figure 4.** Repulsive energy change between cylindrical particles in end-to-end ( $I$ ) configuration; (a) at constant separation distance of  $d/a = 1.0$  with surface potential changes, (b) at constant surface potential of  $\tilde{\psi}_0 = 1.0$  with separation distances.

screening length and surface potential (Figure 4(a)), which is similar to the previous results of parallel configuration. At a constant separation distance, the repulsive energy also reduced with shrinkage of Debye length (Figure 4(b)). Reduction of repulsive energy with increase of ionic strength is commonly observed in most colloidal system, which is driven by screening of charged surface. The repulsive energy and separation distance showed log-linear relation which generally suggested in the repulsion between flat surfaces.<sup>19</sup>

When the cylindrical particles were aligned in an end-to-center ( $T$ ) configuration, the interacting surfaces were the cross-sectional area of cylinder and its orthogonal projection to the cylinder wall. The interacting surface area is same to that of  $I$  configuration,  $\pi a^2$ . However, the surface elements are a little more separated comparing to those of the parallel planes in the  $I$  configuration due to the curvature of cylinder. This extended separation distance of each interacting surface element reduces the repulsive energy. Therefore, total repulsion energy between these two surfaces should be slightly lowered comparing to the case of  $I$  configuration. In Figure 5, the repulsive energy plots were present with the variations of surface potential and the separation distance. All the results were similar to those of  $I$  configuration, however, the magnitudes of the repulsive energy were lowered.

Finally, repulsive energies between crossed cylinders ( $X$  configuration) were calculated. In this case, distances bet-

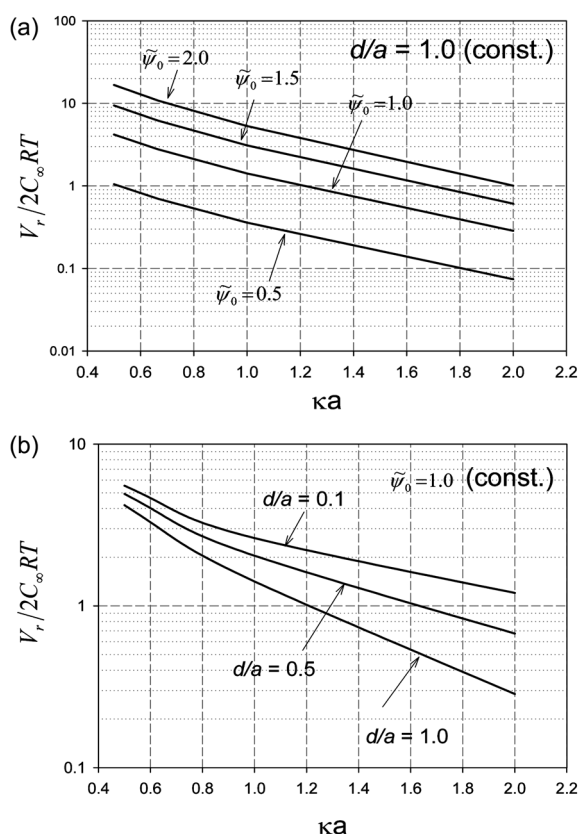


**Figure 5.** Repulsive energy change between cylindrical particles in end-to-center ( $T$ ) configuration; (a) at constant separation distance of  $d/a = 1.0$  with surface potential changes, (b) at constant surface potential of  $\tilde{\psi}_0 = 1.0$  with separation distances.

ween interacting surface elements changes at every point, so does the potential profile. The interacting surface area is  $4a^2$ . The mean separation distance between surface elements is maximized, which minimizes the interaction energy though the interacting surface area is larger than those of  $I$  or  $T$  configurations. The magnitude of the repulsive energy of crossed configuration is lowest among those of all canonical configurations. The repulsive energies at crossed configuration with variation of surface potential and separation distance are shown in Figure 6. As observed before, the repulsive energy reduced when both the surface potential and Debye screening length were lowered.

The magnitudes of repulsive energies of each configuration were compared with the variance of separation distances in Figure 7(a). At a constant surface potential of  $\tilde{\psi}_0 = 1.0$  and constant Debye screening length of  $\lambda_D/a = 1.0$ , the electrostatic repulsive energy increased in the sequence of  $V_r(I) > V_r(T) > V_r(H) > V_r(X)$ . This order of repulsive energy reduction with respect to the configuration agrees with previous results of analytical solution.<sup>6,21</sup> An insight on this repulsive energy changes with the configuration reveals that the mean distance between differential surface elements increases along above sequence. In other words, the repulsive energy is highly affected by the curvature of surfaces. From the comparison between  $I$  and  $T$  configuration results, it is clear that the curved surface would reduce repulsive

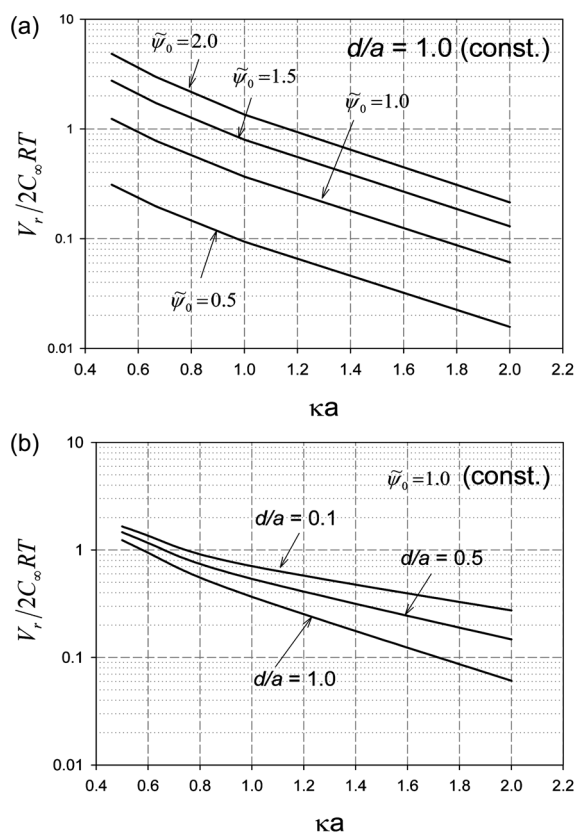


**Figure 6.** Repulsive energy change between crossed cylindrical particles ( $X$  configuration); (a) at constant separation distance of  $d/a = 1.0$  with surface potential changes, (b) at constant surface potential of  $\tilde{\psi}_0 = 1.0$  with separation distances.

energy when the interacting surface area is same. In addition, the more curved surface would have lower repulsive energy even though the interacting surface area is larger than that of less curved ones (compare the surface area of  $H$  and  $X$ ). This curvature effect agrees with the previous reports on the electrical repulsion force between cylinder and sphere<sup>14</sup> and the osmotic pressure decrease in a curved surface.<sup>21</sup> It is notable that above sequence of magnitude would change in a practical system. In real colloidal system containing cylindrical particles, the repulsive energy  $V_r(H)$  would be much larger than those of other configurations because the interacting surface area increase as much as the aspect ratio. For example, a plant virus of tobacco mosaic virus would have aspect ratio of  $\sim 33$  which would result in overwhelming magnitude of  $V_r(H)$  than that of any other configuration. However, the electrical repulsive energy of other configurations would not be influenced by the aspect ratio since the interacting surface area would not change.

In Figure 7(b), the repulsive energy variation of each canonical configuration with respect to surface potential is present. The solid and broken lines represent the repulsive energies at a constant surface potential of  $\tilde{\psi}_0 = 1.0$  and  $\tilde{\psi}_0 = 2.0$ , respectively. All the values were calculated at the same separation distance of  $d/a = 1.0$ . The repulsive energy decays with decrease of Debye screening length regardless to the canonical configuration. This decay is reasonable

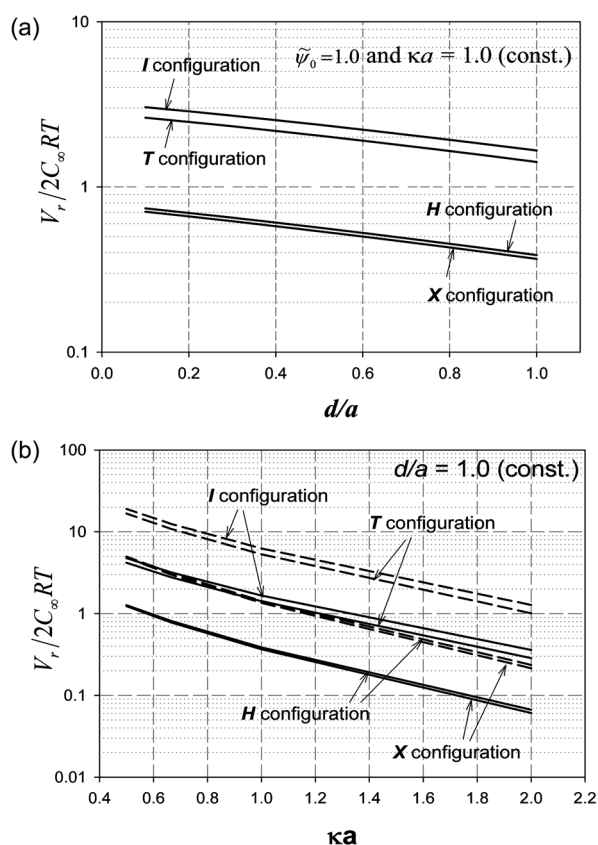


**Figure 7.** Comparison of the repulsive energies between each configuration; (a) Repulsive energy changes with respect to the dimensionless separation distance,  $d/a$  at the same surface potential and Debye length; (b) Repulsive energies of each configuration against Debye length ( $\kappa a$ ) at constant separation distance of  $d/a = 1.0$  (solid line  $\tilde{\psi}_0 = 1.0$ , broken line  $\tilde{\psi}_0 = 2.0$ .)

considering the weaker overlapping takes place with decrease of Debye screening length. In addition, the increased surface potential fastened reduction of repulsive energy. It is due to the counter ion condensation is easier to be happened as the surface potential increases,<sup>22</sup> which makes the potential distribution decays faster.

### Conclusions

The electrostatic repulsion between two finite cylindrical particles is highly dependent on the configurations. Under the Derjaguin approximation, the magnitude of repulsive energy is in the order of  $V_r(I) > V_r(T) > V_r(H) > V_r(X)$ . This

repulsive energy decrease is due to the changes of surface curvature, which affect mean separation distance between interacting surfaces. As the interacting surfaces are getting curved, the repulsion energy decreases because the mean distance between interacting surface elements is getting longer. The repulsive energy is also reduced with decrease of the surface potential and Debye screening length. These results are expected to be applicable in manipulation and analysis of many anisotropic colloid systems that commonly used in modern engineering processes.

**Acknowledgements.** This work was supported by Korea Science and Engineering Foundation (Grant number: KOSEF 2007-8-1158).

### References

- Zareie, M. H.; Xu, X.; Cortie, M. B. *Small* **2007**, *3*, 139.
- Gole, A.; Orendorff, C. J.; Murphy, C. J. *Langmuir* **2004**, *20*, 7117.
- Lee, S.-W.; Mao, C.; Flynn, C. E.; Belcher, A. M. *Science* **2002**, *296*, 892.
- Royston, E.; Lee, S.-Y.; Culver, J. M.; Harris, M. T. *J. Coll. Interface Sci.* **2006**, *298*, 706.
- Bhattacharjee, S.; Chen, J. Y.; Elimelech, M. *Colloids Surfaces A* **2000**, *165*, 143.
- Halle, B. *J. Chem. Phys.* **1995**, *102*, 7338.
- Yoon, B. J.; Kim, S. *J. Coll. Interface Sci.* **1989**, *128*, 275.
- Brenner, S. L.; McQuarrie, D. A. *Biophys. J.* **1973**, *13*, 301.
- Parsegian, V. A.; Brenner, S. L. *Nature* **1976**, *259*, 632.
- Chapot, D.; Bocquet, L.; Trizac, E. *J. Colloid Interface Sci.* **2005**, *285*, 609.
- Hsu, J.-P.; Jiang, J.-M.; Tseng, S. *Colloids Surfaces B* **2003**, *27*, 49.
- Harries, D. *Langmuir* **1998**, *14*, 3149.
- Ospeck, M.; Fraden, S. *J. Chem. Phys.* **1998**, *109*, 9166.
- Gu, Y. *J. Coll. Interface Sci.* **2000**, *231*, 199.
- Hiemenz, P. C.; Rajagopalan, R. *Principles of Colloid and Surface Chemistry*; Marcel Dekker: New York, U.S.A., 1997; p 502.
- Deggelmann, M.; Graf, C.; Hagenbüchle, M.; Hoss, U.; Johner, C.; Kramer, H.; Martin, C.; Weber, R. *J. Phys. Chem.* **1994**, *98*, 364.
- Lee, S.-Y.; Culver, J. N.; Harris, M. T. *J. Coll. Interface Sci.* **2006**, *297*, 554.
- Yang, S. M.; Park, O. O. *Fundamentals of Microstructural Fluid Flow*; Mineumsa: Seoul, Korea, 1997; p 405.
- Hunter, R. J. *Foundations of Colloid Science*; Oxford: New York, U.S.A., 1989; p 191.
- Israelachvili, J. *Intermolecular and Surface Forces*; Academic Press: London, U.K., 1991; p 161.
- Hsu, J.-P.; Yu, H.-Y.; Tseng, S. *J. Phys. Chem. B* **2006**, *110*, 25007.
- Hsu, J.-P.; Yu, H.-Y.; Tseng, S. *J. Phys. Chem. B* **2006**, *110*, 7600.